

P9 Distributed Image Reconstruction for the new Radio Interferometers

Jonas Schwammberger

April 5, 2019

Abstract

Contents

| | | |
|----------|--|-----------|
| 1 | Angular Resolution in Radio Astronomy | 1 |
| 1.1 | Radio Interferometric Inverse Problem | 1 |
| 1.2 | Image Reconstruction | 2 |
| 1.2.1 | Theory of Compressed Sensing | 2 |
| 1.2.2 | State of the art | 2 |
| 1.2.3 | Large scale Reconstruction Problem of MeerKAT | 2 |
| 1.3 | Image Reconstruction | 2 |
| 1.4 | State of the art Deconvolution algorithms | 2 |
| 2 | Image Reconstruction for Radio Interferometers | 3 |
| 2.1 | Distributed Image Reconstruction | 4 |
| 2.2 | First steps towards a distributed Algorithm | 4 |
| 3 | Distributing the Image Reconstruction | 5 |
| 3.1 | Distributed Gridder: The IDG algorithm | 5 |
| 3.2 | Distributed Deconvolution: Coordinate Descent | 6 |
| 4 | Conclusion | 7 |
| 5 | attachment | 10 |
| 6 | Larger runtime costs for Compressed Sensing Reconstructions | 11 |
| 6.1 | CLEAN: The Major Cycle Architecture | 12 |
| 6.2 | Compressed Sensing Architecture | 12 |
| 6.3 | Hypothesis for reducing costs of Compressed Sensing Algorithms | 13 |
| 6.4 | State of the art: WSCLEAN Software Package | 13 |
| 6.4.1 | W-Stacking Major Cycle | 13 |
| 6.4.2 | Deconvolution Algorithms | 13 |
| 6.5 | Distributing the Image Reconstruction | 13 |
| 6.5.1 | Distributing the Non-uniform FFT | 13 |
| 6.5.2 | Distributing the Deconvolution | 13 |
| 7 | Handling the Data Volume | 13 |
| 7.1 | Fully distributed imaging algorithm | 14 |
| 8 | Ehrlichkeitserklärung | 15 |

1 Angular Resolution in Radio Astronomy

Astronomy, Observation of the universe. Higher and higher angular resolution.

Radio Astronomy, single antenna dishes are too expensive

Radio interferometers use several antennas together.

But the problem is that Radio Interferometers do not measure the sky image directly. Instead, they measure Fourier Components.

The inverse Problem

1.1 Radio Interferometric Inverse Problem

Inverse Problem, We have measurements and want to find the image matching the measurements. Incomplete, there are potentially infinite number of images fitting the measurements. This forms an Ill-Posed inverse problem.

Solving this ill posed inverse problem with image reconstruction

Radio Interferometers measure Fourier Components of the Sky. We have a Fourier relationship between measurements and image.

Image reconstruction problem shown in figure 1 Measurements in the Fourier Domain in figure 1a. Each dot represents a measurement of the Radio Interferometer. Incomplete, we do have holes in the UV space. But also a very large number of measurements. We have areas with a high sample density. Reconstructed image 1b

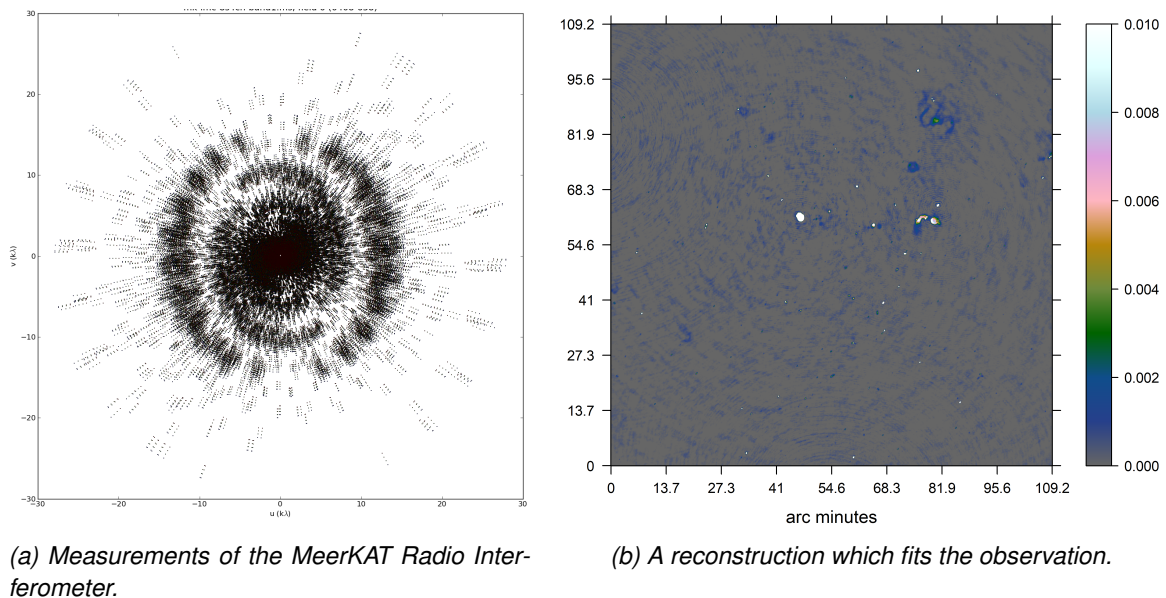


Figure 1: The Image Reconstruction Problem

Overdetermined problem, we have magnitudes more Visibilities than Pixels in the image. But noise and holes in the

Or more formally in equation (1.1)

$$V(u, v, w) = \iint \frac{I(x, y)}{\sqrt{1 - x^2 - y^2}} e^{2\pi i [ux + vy + w(\sqrt{1 - x^2 - y^2} - 1)]} dx dy \quad (1.1)$$

3d Fourier Relationship.

w-projection. Our

1.2 Image Reconstruction

Whole system. From measurements to image reconstruction contains many different steps. In this project, we concern ourselves with the image reconstruction

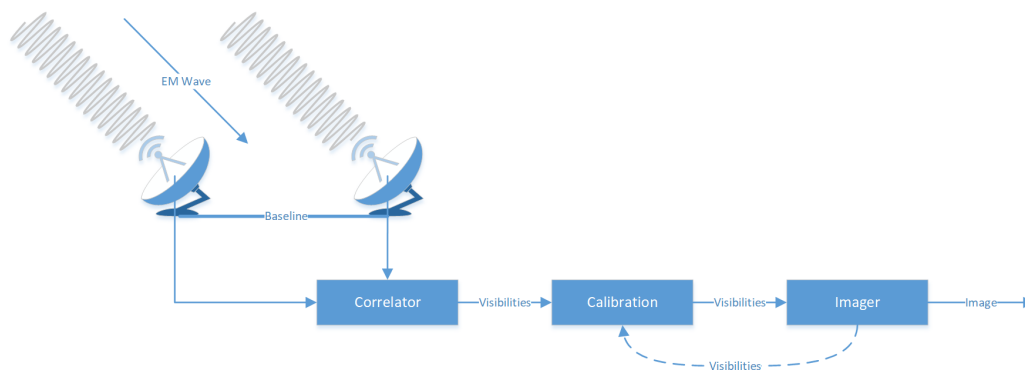


Figure 2: Interferometer System

Calibration is not directly Bad calibration can introduce a special error in the image.

Different ways of formulating the image reconstruction problem: Interpolating the missing Visibilities Deconvolution Finding an image which fits the measurements

1.2.1 Theory of Compressed Sensing

1.2.2 State of the art

1.2.3 Large scale Reconstruction Problem of MeerKAT

New class of radio interferometers produce an ever increasing number of data.

1.3 Image Reconstruction

1.4 State of the art Deconvolution algorithms

CLEAN

Compressed Sensing

What is a deconvolution algorithm

2 Image Reconstruction for Radio Interferometers

In Astronomy, instruments with higher angular resolution allows us to measure ever smaller structures in the sky. For Radio frequencies, the angular resolution is bound to the antenna dish diameter, which puts practical and financial limitations on the highest possible angular resolution. Radio Interferometers get around this limitation by using several smaller antennas instead. Together, they act as a single large antenna with higher angular resolution at lower financial costs compared to single dish instruments.

Each antenna pair of an Interferometer measures a single Fourier component of the observed image. We can retrieve the image by calculating the Fourier Transform of the measurements. However, since the Interferometer only measures an incomplete set of Fourier components, the resulting image is "dirty", convolved with a Point Spread Function (*PSF*). Calculating the Fourier Transform is not enough. To reconstruct the from an Interferometer image, an algorithm has to find the observed image with only the dirty image and the *PSF* as input. It has to perform a deconvolution. The difficulty lies in the fact that there are potentially many valid deconvolutions for a single measurement, and the algorithm has to decide for the most likely one. How similar the truly observed image and the reconstructed images are depends largely on the deconvolution algorithm.

State-of-the-art image reconstructions use the Major Cycle architecture (shown in Figure 3), which contains three operations: Gridding, FFT and Deconvolution.

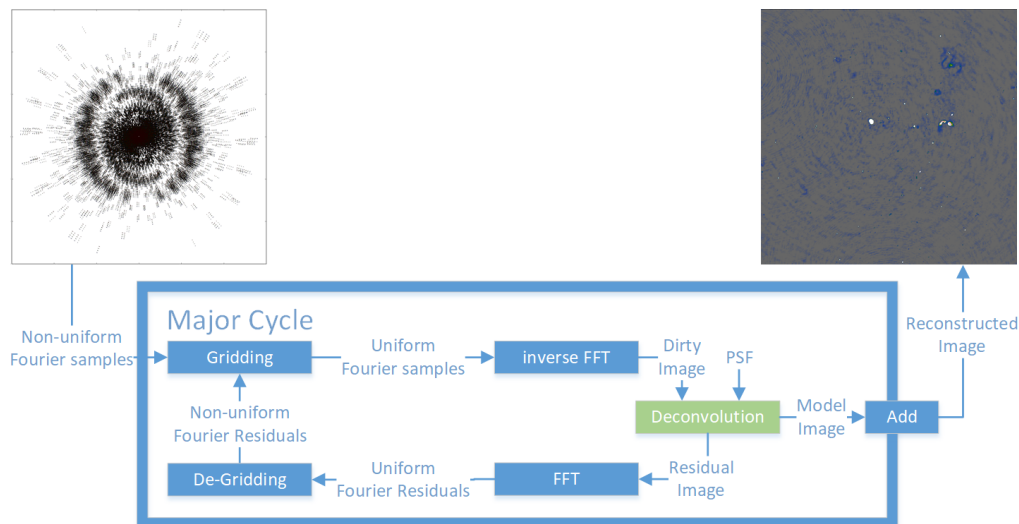


Figure 3: The Major Cycle Architecture of image reconstruction algorithms

The first operation in the Major Cycle, Gridding, takes the non-uniformly sampled Fourier measurements from the Interferometer and interpolates them on a uniformly spaced grid. The uniform grid lets us use FFT to calculate the inverse Fourier Transform and we arrive at the dirty image. A deconvolution algorithm takes the dirty image plus the *PSF* as input, producing the deconvolved "model image", and the residual image as output. At this point, the reverse operations get applied to the residual image. First the FFT and then De-gridding, arriving at the non-uniform Residuals. The next Major Cycle begins with the non-uniform Residuals as input. The cycles are necessary, because the Gridding and Deconvolution operations are only approximations. Over several cycles, we reduce the errors introduced by the approximate Gridding and Deconvolution. The final, reconstructed image is the addition of all the model images of each Major Cycle.

2.1 Distributed Image Reconstruction

New Interferometer produce an ever increasing number of measurements, creating ever larger reconstruction problems. A single image can contain several terabytes of Fourier measurements. Handling reconstruction problems of this size forces us to use distributed computing. However, state-of-the-art Gridding and Deconvolution algorithms only allow for limited distribution. How to scale the Gridding and Deconvolution algorithms to large problem sizes is still an open question.

Recent developments make a distributed Gridder and a distributed Deconvolution algorithm possible. Veeneboer et al[2] found an input partitioning scheme, which allowed them to perform the Gridding on the GPU. The same partitioning scheme can potentially be used to distribute the Gridding onto multiple machines. For Deconvolution, there exist parallel implementations for certain algorithms like MORESANE[3]. These can be used as a basis for a fully distributed image reconstruction.

In this project, we want to make the first steps towards an image reconstruction algorithm, which is distributed from end-to-end, from Gridding up to and including deconvolution. We create our own distributed Gridding and Deconvolution algorithms, and analyse the bottlenecks that arise.

2.2 First steps towards a distributed Algorithm

In this project, we make the first steps towards a distributed Major Cycle architecture (shown in figure 3) implemented C#. We port Veeneboer et al's Gridder, which is written in C++, to C# and modify it for distributed computing. We implement a simple deconvolution algorithm based on the previous project and create a first, non-optimal distributed version of it.

In the next step, we create a more sophisticated deconvolution algorithm based on the shortcomings of the first implementation. We use simulated and real-world observations of the MeerKAT Radio Interferometer and measure its speed up. We identify the bottlenecks of the current implementation and explore further steps.

From the first lessons, we continually modify the distributed algorithm and focus on decreasing the need for communication between the nodes, and increase the overall speed up compared to single-machine implementations. Possible Further steps:

- Distributed FFT
- Replacing the Major Cycle Architecture
- GPU-accelerated Deconvolution algorithm.

A state-of-the-art reconstruction algorithm has to correct large number of measurement effects arising from the Radio Interferometer. Accounting for all effects is out of the scope for this project. We make simplifying assumptions, resulting in a proof-of-concept algorithm.

Speedups are still relevant

3 Distributing the Image Reconstruction

Distributing the whole image reconstruction. So far, only parts were distributed. First time that end to end, everything gets distributed.

OpenMPI

Gridding and Deconvolution

3.1 Distributed Gridder: The IDG algorithm

Veeneboer et al[2] developed the Image Domain Gridder. It uses Subgrids and solves each subgrid separately. It is in the image domain, because it can do Radio Interferometer specific corrections efficiently. Furthermore, it leads to a structure which is primed for GPU processing. We use this algorithm to distribute the gridding.

W-Projection, Spheroidal are convolutions in the Fourier space.

The figure 4 shows the different parts of the image domain algorithm.

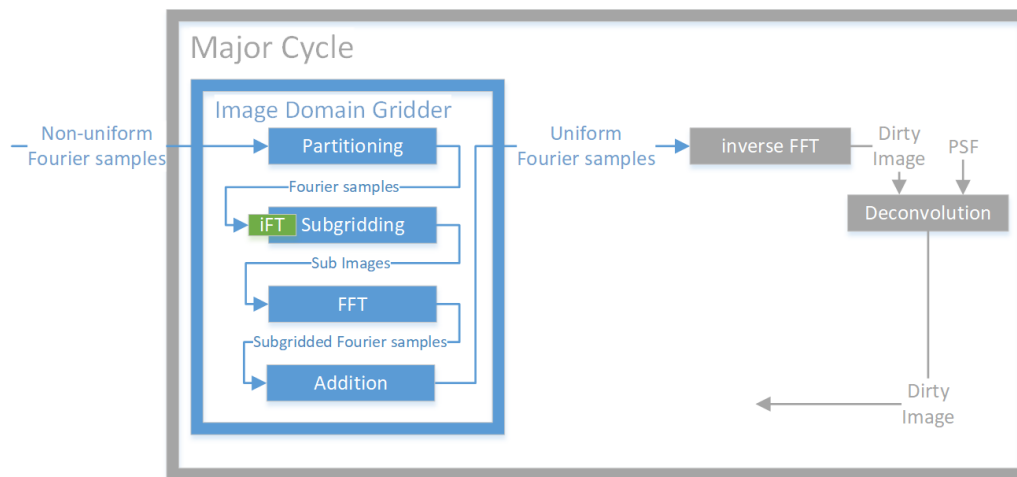


Figure 4: Image Domain Gridder in the Major Cycle Architecture

Algorithm

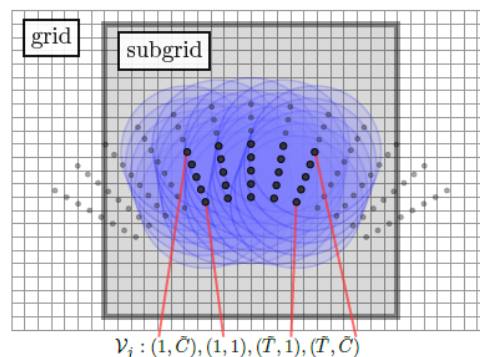


Figure 5: Subgrid

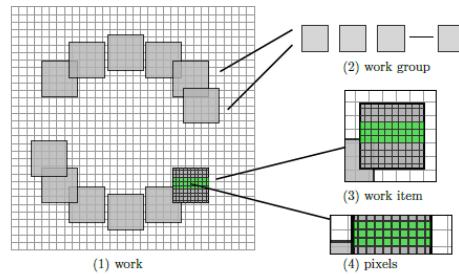


Figure 6: parallel

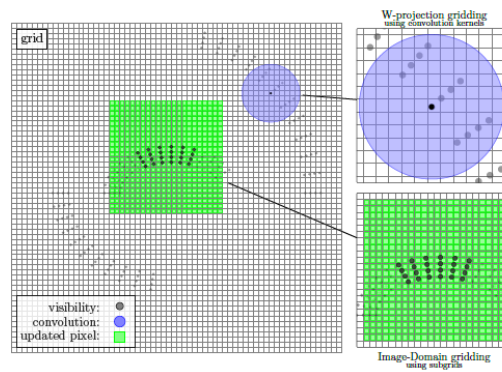


Figure 7: Image Domain Gridder in the Major Cycle Architecture

3.2 Distributed Deconvolution: Coordinate Descent

4 Conclusion

References

- [1] Tim J Cornwell, Kumar Golap, and Sanjay Bhatnagar. The noncoplanar baselines effect in radio interferometry: The w -projection algorithm. IEEE Journal of Selected Topics in Signal Processing, 2(5):647–657, 2008.
- [2] Bram Veenboer, Matthias Petschow, and John W Romein. Image-domain gridding on graphics processors. In 2017 IEEE International Parallel and Distributed Processing Symposium (IPDPS), pages 545–554. IEEE, 2017.
- [3] Arwa Dabbech, Chiara Ferrari, David Mary, Eric Slezak, Oleg Smirnov, and Jonathan S Kenyon. More-sane: Model reconstruction by synthesis-analysis estimators-a sparse deconvolution algorithm for radio interferometric imaging. Astronomy & Astrophysics, 576:A7, 2015.
- [4] AR Offringa, Benjamin McKinley, Natasha Hurley-Walker, FH Briggs, RB Wayth, DL Kaplan, ME Bell, Lu Feng, AR Neben, JD Hughes, et al. Wsclean: an implementation of a fast, generic wide-field imager for radio astronomy. Monthly Notices of the Royal Astronomical Society, 444(1):606–619, 2014.
- [5] Luke Pratley, Melanie Johnston-Hollitt, and Jason D McEwen. A fast and exact w -stacking and w -projection hybrid algorithm for wide-field interferometric imaging. arXiv preprint arXiv:1807.09239, 2018.

List of Figures

| | | |
|---|---|----|
| 1 | The Image Reconstruction Problem | 1 |
| 2 | Interferometer System | 2 |
| 3 | The Major Cycle Architecture of image reconstruction algorithms | 3 |
| 4 | Image Domain Gridder in the Major Cycle Architecture | 5 |
| 5 | Subgrid | 5 |
| 6 | parallel | 6 |
| 7 | Image Domain Gridder in the Major Cycle Architecture | 6 |
| 8 | The Major Cycle Architecture | 12 |
| 9 | State-of-the-art Compressed Sensing Reconstruction Architecture | 12 |

List of Tables

5 attachment

6 Larger runtime costs for Compressed Sensing Reconstructions

The MeerKAT instrument produces a new magnitude of data volume. An image with several million pixels gets reconstructed from billions of Visibility measurements. Although MeerKAT measures a large set of Visibilities, the measurements are still incomplete. We do not have all the information available to reconstruct an image. Essentially, this introduces "fake" structures in the image, which a reconstruction algorithm has to remove. Additionally, the measurements are noisy.

We require an image reconstruction algorithm which removes the "fake" structures from the image, and removes the noise from the measurements. The large data volume of MeerKAT requires the algorithm to be both scalable and distributable. Over the years, several reconstruction algorithms were developed, which can be separated into two classes: Algorithms based on CLEAN, which are cheaper to compute and algorithms based on Compressed Sensing, which create higher quality reconstructions.

CLEAN based algorithms represent the reconstruction problem as a deconvolution. First, they calculate the "dirty" image, which is corrupted by noise and fake image structures. The incomplete measurements essentially convolve the image with a Point Spread Function (*PSF*). CLEAN estimates the *PSF* and searches for a deconvolved version of the dirty image. In each CLEAN iteration, it searches for the highest pixel in the dirty image, subtracts a fraction *PSF* at the location. It adds the fraction to the same pixel location of a the "cleaned" image. After several iterations, the cleaned image contains the deconvolved version of the dirty image. CLEAN accounts for noise by stopping early. It stops when the highest pixel value is smaller than a certain threshold. This results in a light-weight and robust reconstruction algorithm. CLEAN is comparatively cheap to compute, but does not produce the best reconstructions and is difficult to distribute on a large scale.

Compressed Sensing based algorithms represent the reconstruction as an optimization problem. They search for the optimal image which is as close to the Visibility measurements as possible, but also has the smallest regularization penalty. The regularization encodes our prior knowledge about the image. Image structures which were likely measured by the instrument result in a low regularization penalty. Image structures which were likely introduced by noise or the measurement instrument itself result in high penalty. Compressed Sensing based algorithms explicitly handle noise and create higher quality reconstructions than CLEAN. State-of-the-art Compressed Sensing algorithms show potential for distributed computing. However, they currently do not scale on MeerKATs data volume. They require too many computing resources compared to CLEAN based algorithms.

This project searches for a way to reduce the runtime costs of Compressed Sensing based algorithms. One reason for the higher costs is due to the non-uniform FFT Cycle. State-of-the-art CLEAN and Compressed Sensing based algorithms both use the non-uniform FFT approximation in a cycle during reconstruction. The interferometer measures the Visibilities in a continuous space in a non-uniform pattern. The image is divided in a regularly spaced, discrete pixels. The non-uniform FFT creates an approximate, uniformly sampled image from the non-uniform measurements. Both, CLEAN and Compressed Sensing based algorithms use the non-uniform FFT to cycle between non-uniform Visibilities and uniform image. However, a Compressed Sensing algorithm requires more non-uniform FFT cycles for reconstruction.

CLEAN and Compressed Sensing based algorithms use the non-uniform FFT in a similar manner. However, there are slight differences in the architecture. This project hypothesises that The previous project searched for an alternative to the non-uniform FFT cycle. Although there are alternatives, there is currently no replacement which leads to lower runtime costs for Compressed Sensing. Current research is focused on reducing the number of non-uniform FFT cycles for Compressed Sensing algorithms.

CLEAN based algorithms use the Major Cycle Architecture for reconstruction. Compressed Sensing based algorithms use a similar architecture, but with slight modifications. Our hypothesis is that we may reduce the number of non-uniform FFT cycles for Compressed Sensing by using CLEAN's Major Cycle Architecture.

6.1 CLEAN: The Major Cycle Architecture

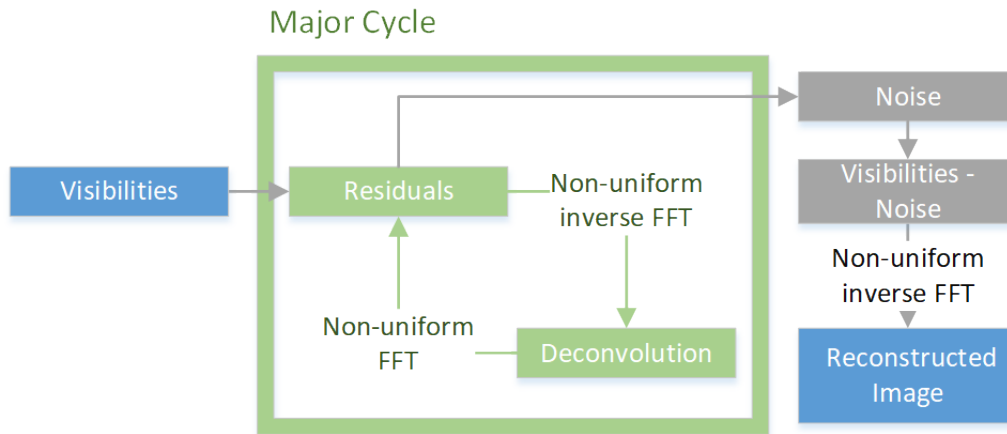


Figure 8: The Major Cycle Architecture

Figure 8 depicts the Major Cycle Architecture used by CLEAN algorithms. First, the Visibilities get transformed into an image with the non-uniform FFT. The resulting dirty image contains the corruptions of the measurement instrument and noise. A deconvolution algorithm, typically CLEAN, removes the corruption of the instrument with a deconvolution. When the deconvolution stops, it should have removed most of the observed structures from the dirty image. The rest, mostly noisy part of the dirty image gets transformed back into residual Visibilities and the cycle starts over.

In the Major Cycle Architecture, we need several deconvolution attempts before it has distinguished the noise from the measurements. Both the non-uniform FFT and the deconvolution are approximations. By using the non-uniform FFT in a cycle, it can reconstruct an image at a higher quality. For MeerKAT reconstruction with CLEAN, we need approximately 4-6 non-uniform FFT cycles for a reconstruction.

6.2 Compressed Sensing Architecture

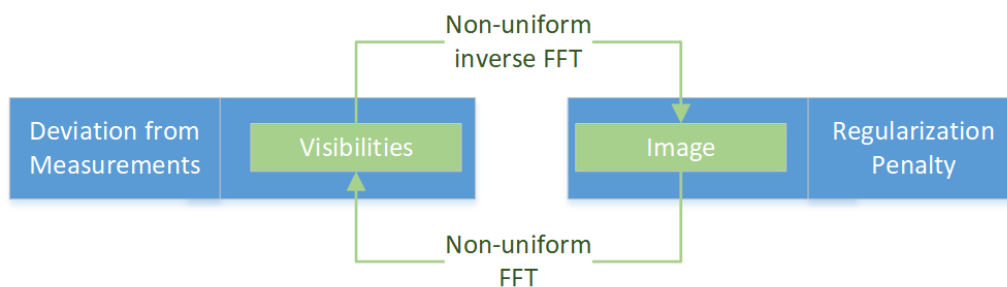


Figure 9: State-of-the-art Compressed Sensing Reconstruction Architecture

Figure 9 depicts the architecture used by Compressed Sensing reconstructions. The Visibilities get transformed into an image with the non-uniform FFT approximation. The algorithm then modifies the image so it reduces the regularization penalty. The modified image gets transformed back to Visibilities and the algorithm then minimizes the difference between measured and reconstructed Visibilities. This is repeated until the algorithm converges to an optimum.

In this architecture, state-of-the-art Compressed Sensing algorithms need approximately 10 or more non-uniform FFT cycles to converge. It is one source for the higher runtime costs. For MeerKAT reconstructions

the non-uniform FFT tends to dominate the runtime costs. A CLEAN reconstruction with the Major Cycle Architecture already spends a large part of its time in the non-uniform FFT. Compressed Sensing algorithms need even more non-uniform FFT cycle on top of the "Image Regularization" step being generally more expensive than CLEAN deconvolution. There is one upside in this architecture: State-of-the-art algorithms managed to distribute the "Image Regularization" operation.

6.3 Hypothesis for reducing costs of Compressed Sensing Algorithms

Compressed Sensing Algorithms are not bound to the Architecture presented in section 6.2. For example, we can design a Compressed Sensing based deconvolution algorithm and use the Major Cycle Architecture instead.

Our hypothesis is: We can create a Compressed Sensing based deconvolution algorithm which is both distributable and creates higher quality reconstructions than CLEAN. Because it also uses the Major Cycle architecture, we reckon that the Compressed Sensing deconvolution requires a comparable number of non-uniform FFT cycles to CLEAN. This would result in a Compressed Sensing based reconstruction algorithm with similar runtime costs to CLEAN, but higher reconstruction quality and higher potential for distributed computing.

6.4 State of the art: WSCLEAN Software Package

6.4.1 W-Stacking Major Cycle

6.4.2 Deconvolution Algorithms

CLEAN MORESANE

6.5 Distributing the Image Reconstruction

6.5.1 Distributing the Non-uniform FFT

6.5.2 Distributing the Deconvolution

7 Handling the Data Volume

The new data volume is a challenge to process for both algorithms and computing infrastructure. Push for parallel and distributed algorithms. For Radio Interferometer imaging, we require specialized algorithms. The two distinct operations, non-uniform FFT and Deconvolution, were difficult algorithms for parallel or distributed computing.

The non-uniform FFT was historically what dominated the runtime []. Performing an efficient non-uniform FFT for Radio Interferometers is an active field of research[4, 5], continually reducing the runtime costs of the operation. Recently, Veeneboer et al[2] developed a non-uniform FFT which can be fully executed on the GPU. It speeds up the most expensive operation.

In Radio Astronomy, CLEAN is the go-to deconvolution algorithm. It is light-weight and compared to the non-uniform FFT, a cheap algorithm. It is also highly iterative, which makes it difficult for effective parallel or distributed implementations. However, compressed sensing based deconvolution algorithms can be developed with distribution in mind.

7.1 Fully distributed imaging algorithm

Current imaging algorithms push towards parallel computing with GPU acceleration. But with Veeneboer et al's non-uniform FFT and a compressed sensing based deconvolution, we can go a step further and create a distributed imaging algorithm.

8 Ehrlichkeitserklärung

Hiermit erkläre ich, dass ich die vorliegende schriftliche Arbeit selbstständig und nur unter Zuhilfenahme der in den Verzeichnissen oder in den Anmerkungen genannten Quellen angefertigt habe. Ich versichere zudem, diese Arbeit nicht bereits anderweitig als Leistungsnachweis verwendet zu haben. Eine Überprüfung der Arbeit auf Plagiate unter Einsatz entsprechender Software darf vorgenommen werden.

Windisch, April 5, 2019

Jonas Schwammberger